Investigating the Interactions of Metal Ions, Compounds, and calf-thymus DNA Using UV-Vis Spectroscopy

Austyn S. Barjona, Jacob Alewine, Julia L. Brumaghim

Clemson University

December 19, 2022

Keywords: DNA, Fe(II), Zn(II), dmit, dmise, glutathione, binding constant, UV-Vis

Abstract

Metal ions, such as Fe(II) and Zn(II), have the ability to produce DNA damaging radicals from hydrogen peroxide as seen in the Fenton reaction. The objective of this study is to observe the bindings of these metals and three antioxidant compounds dmit, dmise, and glutathione (see Fig. 1), with calf thymus DNA using UV-Vis spectroscopy. The concentration of CT-DNA was held constant while increasing the concentration of a metal ion or compound. Upon observation, the absorbance of DNA decreased upon the addition of metal ions but increased or decreased to a lesser extent upon the addition of N, N-dimethylimidazole thione (dmit), N, N-dimethylimidazole selone (dmise), dmise, and glutathione (GSH) compounds. For example, in the Zn(II) titration, the absorbance of CT-DNA at 260 nm without the addition of Zn(II) was 0.63 AU while its absorbance after adding 50. μM of Zn(II) was 0.26 AU. In the dmit titration, absorbance of CT-DNA had increased as dmit concentration increased (from 2.3 AU upon addition of 5.0 μM dmit to 2.5 AU upon addition of 10. μM dmit). From this observation, it can be concluded that the relationship of the absorbances between DNA and these small molecules can help determine if DNA binding interactions can occur based on notable shifts in UV-Vis absorbances as well as new drugs to prevent DNA damage.

Introduction

Metal ions Fe(II) and Zn(II) display comparable geometry and structure as well as similar DNA-binding ability.[1] For example, Fe(II) and Zn(II) complexes have been found to interact with DNA through the intercalation binding mode and are efficient as antitumor agents due to their ability to intercalate between DNA base pairs and cytotoxicity of tumor cells respectively.[2-4] In addition, Zn(II) has shown antitumor activity such as decreasing the growth rate of cancer cells in human breast cancer and prostate cancer.[5,6] There are, however, disadvantages to these

metal ions, such as the production of the Fenton Reaction. In this reaction, metal ions are able to react with hydrogen peroxide (H_2O_2) to produce harmful derivatives and radicals in DNA which can lead to cell death in human cells.[7-9] This is caused by one of the unpaired valence electrons from Fe(II) reacting with H_2O_2 to form a hydroxyl radical and oxidants (in Reaction 1 shown below).

$$Fe^{2+} + H_2O_2 \rightarrow Fe^{3+} + {}^{\bullet}OH + OH^- \quad (1)$$

This reaction is destructive to DNA due to radicals being produced. These radicals are shown to bring about damage to DNA at its base and phosphate backbone.[9] Unlike Fe(II), Zn(II) cannot react with hydrogen peroxide to produce the hydroxyl radical, but it can intercalate on DNA and undergo deficiency that may cause growth effects and disorders of the central nervous system.[10, 11] As researchers struggle to design more efficient and specifically targeted therapeutics with fewer side effects, understanding the binding of small molecules to DNA can help develop new drugs that can recognize a specific site or binding of DNA.[12,13] Metal ions as a whole have been considered to be freely diffusible across the nuclear pores, therefore the possibility that metals ions are transported into the nucleus and bound to DNA because of different matters is to be observed.[14]

In order to prevent the formation of these radicals, it is thought that sulfur and selenium-containing antioxidant compounds such as dmit, dmise, and GSH have the ability to bind to the metal ions/compounds before they produce radicals. This however, is usually performed through metal coordination as the presence of a sulfur or selenium atom by itself is not effective for antioxidant activity. Because the sulfur and selenium antioxidants show activity close to expected coordination ratios for these metal ions, metal coordination is the most favorable technique.[8] This is why compounds involving sulfur and selenium in them are used in

the experiments as opposed to solutions with pure sulfur and selenium atoms by themselves. The structures for the antioxidant compounds used in the experiment are shown in Fig. 1 below:

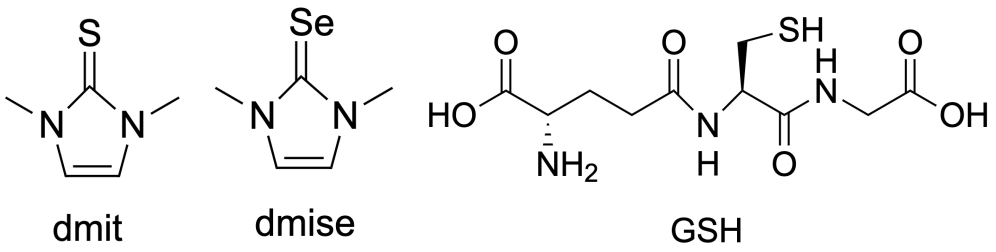

Fig. 1. The structures of the sulfur and selenium compounds (dmit, dmise, and GSH) used in this experiment.

Concerning the antioxidant GSH, it is considered one of the most vital low molecular weight antioxidants synthesized within cells. It is synthesized by the sequential addition of cysteine to glutamate, then glycine.[15] GSH has additional functions other than preventing DNA damage, including detoxification for several toxins and carcinogens, regulation of protein function and helping to preserve immune function. Low levels of GSH are connected with increased risks for cancer, cardiovascular diseases, arthritis and diabetes.[16] Therefore with these properties, it is possible to make use of these antioxidants in order to prevent metal-mediated DNA damage.

Experimental Methods

UV-Vis Spectroscopy

For all experiments, 3-6 mL aliquots of 100 μM CT-DNA were prepared and adjusted with 3-morpholinopropane-1-sulfonic acid (MOPS) buffer and 5 mM NaCl for each experiment. Ternary titrations of CT-DNA and metal ion/compound were achieved, while varying the concentrations of the metal ion/compound to be 2.5 μM, 5.0 μM, 12.5 μM, 25 μM, and 50 μM for each recording with the exception of glutathione, where 5.0 μM, 10 μM, 15 μM, 20 μM, and 25 μM concentrations were used. By using a UV-Vis spectrometer, the absorbances of the combinations of CT-DNA and the metal ions/compounds were used to observe the interactions

between CT-DNA and the molecules. These results were observed between the wavelengths 260-280 nm. Throughout the course of the experiment, 1 mL of 100 µM CT-DNA was mixed with 1 mL of metal ion/complex at increasing concentrations. One titration was performed for Zn(II), two titrations for dmise, three titrations for dmit, and two titrations for GSH. The control groups and the solution ratio added into the cuvette for each titration are presented in Table 1.

Table 1. The control groups and ratios of each titration that were added into the cuvette in order of CT-DNA, metal ion, and antioxidant compound.

Titration	Control(s)	1 mL Ratios with 100 µM CT-DNA
DNA/Zn(II)	CT-DNA only	1:1
DNA/Dmise	CT-DNA only	1:1
DNA/Zn(II) + Dmise	CT-DNA only CT-DNA + Zn(II)	1:1:1
DNA/Dmit	CT-DNA only	1:1
DNA/Zn(II) + Dmit	CT-DNA only CT-DNA + Zn(II)	1:1:1
DNA/Fe(II) + Dmit	CT-DNA only CT-DNA + Fe(II)	1:1:1
DNA/GSH	CT-DNA only	1:1
DNA/Zn(II) + GSH	CT-DNA only CT-DNA + Zn(II)	1:1:1

Determination of the Binding Constant, K_b

The binding constant K_b can determine the binding affinity that is present between CT-DNA and the ligand it reacts with.

$$\frac{1}{A - A_0} = \frac{1}{A_\infty - A_0} + \frac{1}{K(A - A_0)} \times \frac{1}{[L_0]} \quad (1)$$

According to Equation (1) above (where A is equal to the recorded absorbance at varying ligand concentrations, where A_0 is the initial absorbance of CT-DNA at 260 nm, where A_∞ is equal to the final absorbance of CT-DNA bounded with the ligand, and where $[L_0]$ is equal to the ligand concentration), K must be equal to the ratio of the y-intercept over the slope of a double reciprocal plot $\frac{1}{[L_0]}$ vs. $\frac{1}{A-A_0}$, were $\frac{1}{[L_0]}$ is displayed on the x-axis and $\frac{1}{A-A_0}$ is displayed on the y-axis. This ratio for determining K is therefore written as $\frac{\left(\frac{1}{A_\infty - A_0}\right)}{\frac{1}{K(A-A_0)}}$. From this information, double reciprocal plots were constructed to calculate the binding constants for each titration

Results and Discussion

Eight titrations were conducted for the purpose of being able to calculate their binding constants. This will help determine the binding affinity happening between the molecules as well as if the solutions were too concentrated to be able to tell what these binding affinities were. Below are spectra of the eight titrations conducted by performing ternary titrations of the ligand with CT-DNA as well as the double reciprocal plots used to calculate the binding constant:

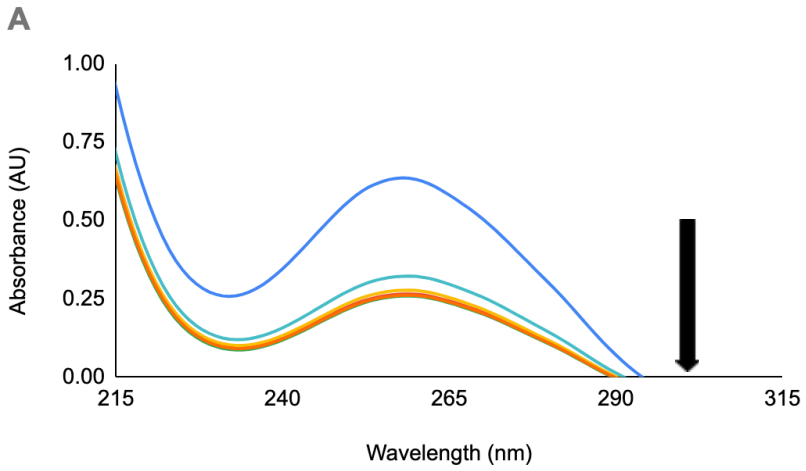

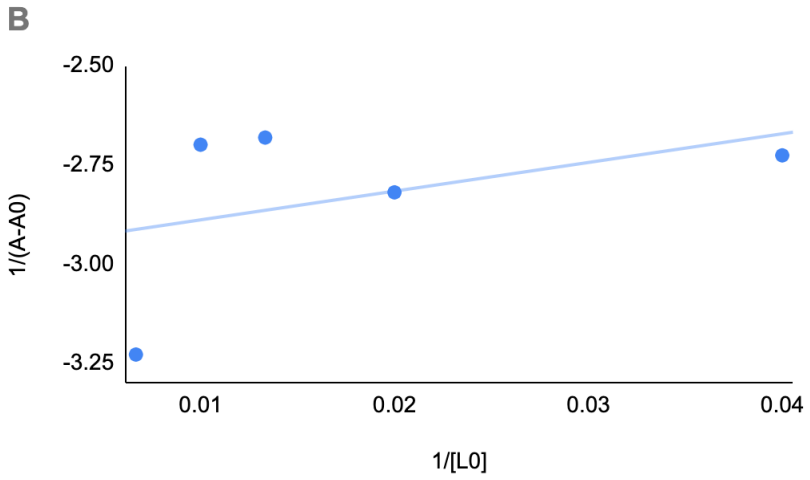

Fig. 2. (A) Absorbances of calf thymus DNA with varying concentrations of Zn(II). The concentrations for the added amounts of Zn(II) are as follows: DNA only (blue), 25 µM Zn(II) (red), 50 µM Zn(II) (yellow), 75 µM Zn(II) (green), 100 µM Zn(II) (orange), 150 µM Zn(II) (turquoise). (B) Double reciprocal plot for the absorbances of calf thymus DNA with varying concentrations of Zn(II). From this data, the binding constant was calculated to be -0.409. The equation was -2.96 + 7.23x and the R^2 value was 0.176.

In the presence of Zn(II), CT-DNA is shown to decrease just as expected (decrease of CT-DNA shown by the arrow in the figure). Therefore, it can be concluded through concentration levels in both titrations that Zn(II) decreases the absorbance of DNA when interacted with it. Additionally, there was a very low correlation between the increasing of Zn(II) concentration when added to the DNA solution. The binding constant was also calculated to be negative. This low correlation and negative constant could have to do with calculating the binding constant using a poor method. Using other techniques to calculate the binding constant could improve the accuracy of the calculations and produce a more correlated plot as well as a positive binding constant.

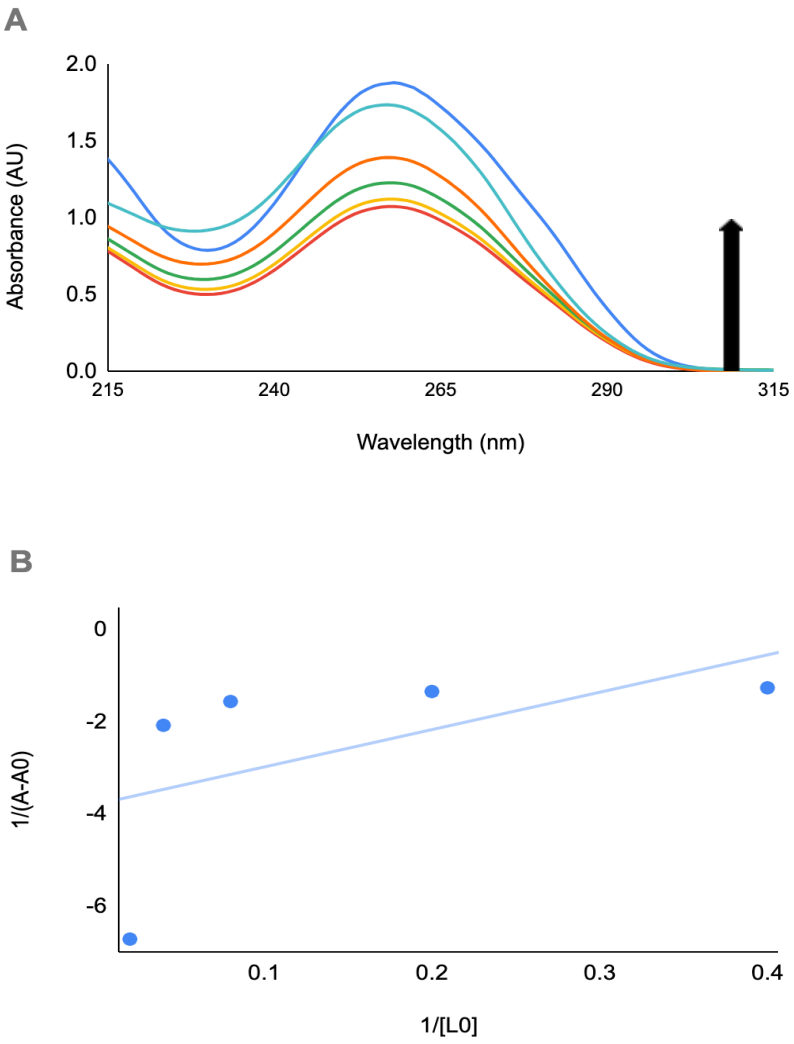

Fig. 3. (A) Absorbances of calf thymus DNA with varying concentrations of dmise. The concentrations of the added amounts of dmise are as follows: DNA Only (blue), 2.5 µM dmise (red) 5.0 µM dmise (yellow), 12.5 µM dmise (green), 25 µM dmise (orange), 50 µM dmise (turquoise). (B) Double reciprocal plot for the absorbances of calf thymus DNA with varying concentrations of dmise. From this data, the binding constant was calculated to be -0.466. The equation was -3.78 + 8.11x and the R^2 value was 0.300.

When dmise alone is added to CT-DNA, its absorbance initially decreases. When the concentration of dmise increases however, the absorbance also increases as indicated by the arrow. Because of this phenomenon, this antioxidant compound is very likely to provide protection to CT-DNA upon the addition of Zn(II) ion solution. Like the previous double reciprocal plot however, the addition of dmise alone did not have much correlation at a

wavelength of 260 nm. The binding constant is a negative number due to the same reason as the previous reciprocal plot (an insufficient method used to calculate the binding constant).

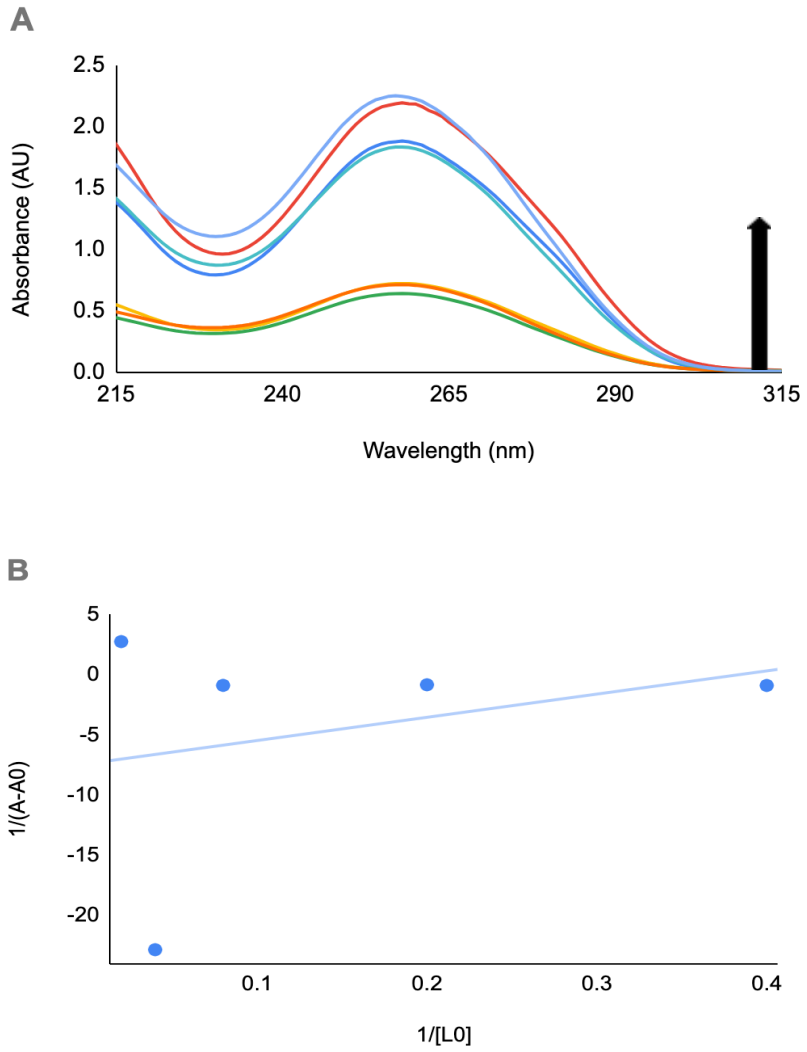

Fig. 4. (A) Absorbances of calf thymus DNA and Zn(II) with varying concentrations of dmise. The added amounts of the ion/complex as well as the concentrations of dmise are as follows: DNA Only (blue), DNA and Zn(II) (red), 2.5 µM dmise (yellow) 5.0 µM dmise (green), 12.5 µM dmise (orange), 25 µM dmise (turquoise), 50 µM dmise (light blue). (B) Double reciprocal plot for the absorbances of calf thymus DNA and Zn(II) with varying concentrations of dmise. From this data, the binding constant was calculated to be -0.311. The equation was -7.37 + 19.3x and the R^2 value was 0.086.

When Zn(II) is bound to CT-DNA before dmise, the Zn(II) ions break down CT-DNA before the dmise interacts with the solution. It does however, generally increase the absorbance of the CT-DNA upon increasing the dmise concentration. Because of this, the gap between the

absorbance of CT-DNA alone and with Zn(II) decreases (see Fig. 2). Concerning the double reciprocal plot, the correlation is very low for the addition of dmise into DNA solution already bound to Zn(II). The binding constant is also negative. The reason for this could once again be due to the method for calculating the binding constant being inefficient.

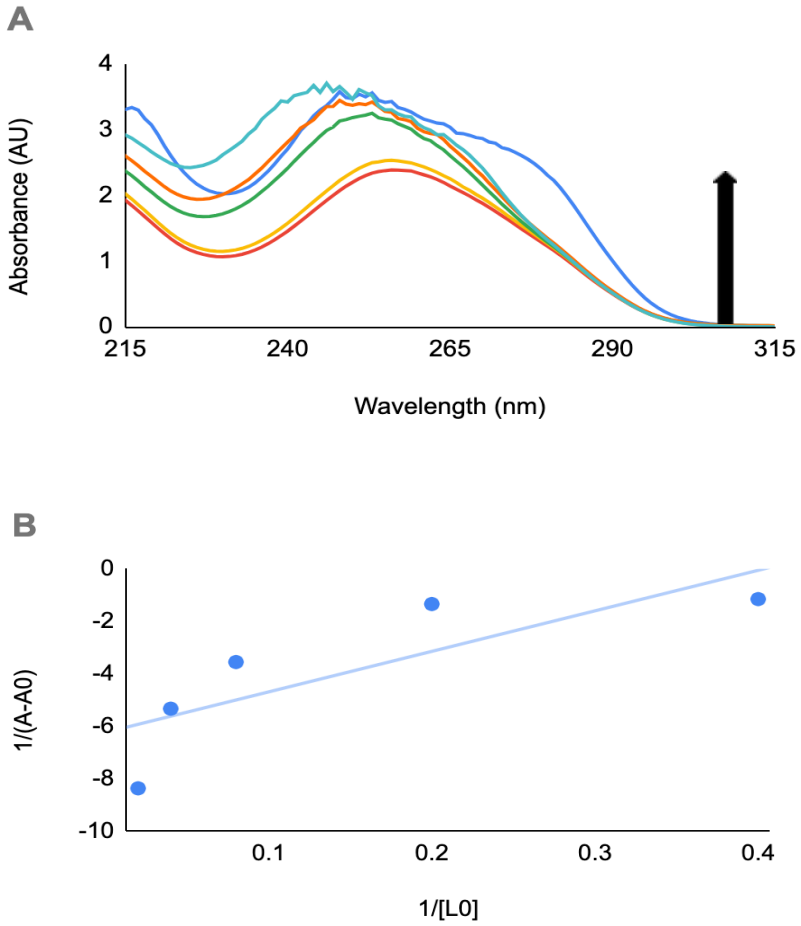

Fig. 5. (A) Absorbances of calf thymus DNA with varying concentrations of dmit. The concentrations of the added amounts of dmit are as follows: DNA Only (blue), 2.5 µM dmit (red) 5.0 µM dmit (yellow), 12.5 µM dmit (green), 25 µM dmit (orange), 50 µM dmit (turquoise). (B) Double reciprocal plot for the absorbances of calf thymus DNA with varying concentrations of dmit. From this data, the binding constant was calculated to be -0.403. The equation was -6.24 + 15.5x and the R^2 value was 0.652.

Like dmise, when dmit alone is added to CT-DNA its absorbance initially decreases, but the absorbance of CT-DNA increases with increasing concentration of dmit as indicated by the arrow. Because of this phenomenon, this dmit is also very likely to provide protection to

CT-DNA upon the addition of Zn(II) ion solution. Unlike dmise however, there is a small amount of noise present between the 250-260 nm for the higher concentrations of dmit (12.5 µM, 25 µM, and 50 µM) despite that dmise titration was at the same concentrations and produced no noise. This is more than likely due to the fact that dmit reacts more vigorously with CT-DNA, as the absorbances are much closer in comparison to the original CT-DNA absorbance to the point of exceeding it (see Fig. 2 for comparison). Therefore, dmit produces much more favorable results when CT-DNA reacts with Zn(II). Concerning the double reciprocal plot, the addition of dmit alone at a wavelength of 260 nm has better correlation, which further proves how strongly the antioxidant compound reacts with CT-DNA. The binding constant, however, is still a negative number due to the reasons as stated earlier (an insufficient method used to calculate the binding constant).

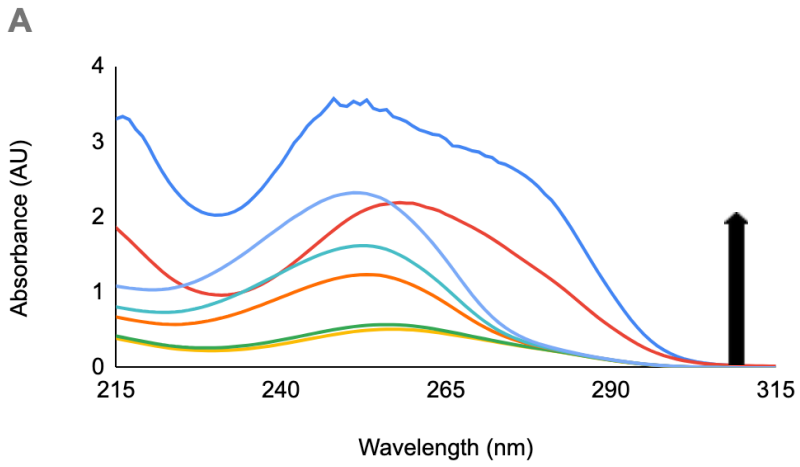

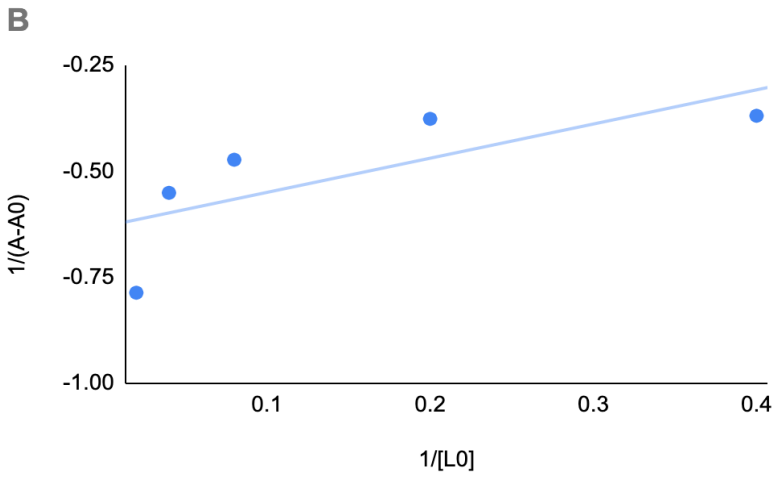

Fig. 6. (A) Absorbances of calf thymus DNA and Zn(II) with varying concentrations of dmit. The added amounts of the ion/complex as well as the concentrations of dmit are as follows: DNA Only (blue), DNA and Zn(II) (red), 2.5 µM dmit (yellow) 5.0 µM dmit (green), 12.5 µM dmit (orange), 25 µM dmit (turquoise), 50 µM dmit (light blue). (B) Double reciprocal plot for the absorbances of calf thymus DNA and Zn(II) with varying concentrations of dmit. From this data, the binding constant was calculated to be -0.782. The equation was -0.63 + 0.806x and the R^2 value was 0.549.

Like with dmise in Fig. 4, when Zn(II) is bound to CT-DNA before dmit, the Zn(II) ions break down CT-DNA before the dmit interacts with the solution. Also like dmise, the dmit generally increases the absorbance of the CT-DNA. Because of this, the gap between the absorbance of CT-DNA alone and with Zn(II) decreases (see Fig. 2). Concerning the double reciprocal plot, the correlation is slightly lower compared to dmit by itself, which could be due to the addition of Zn(II) ion beforehand. The binding constant is also negative, due to reasons previously mentioned (an insufficient method used to calculate the binding constant).

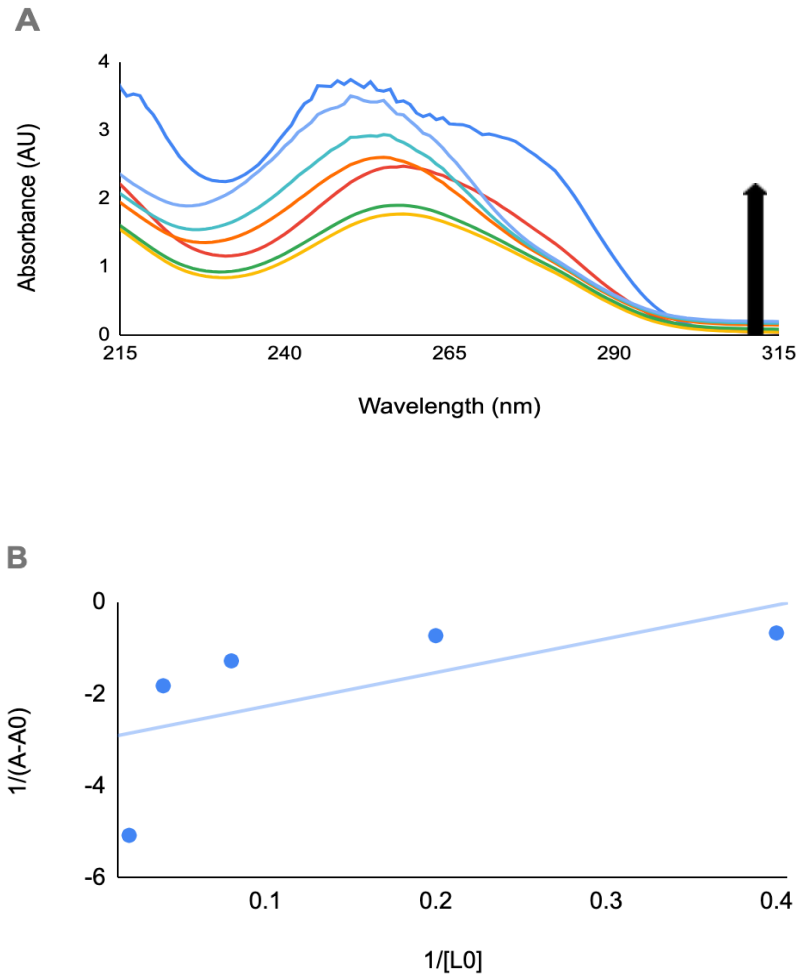

Fig. 7. (A) Absorbances of calf thymus DNA and Fe(II) with varying concentrations of dmit. The added amounts of the ion/complex as well as the concentrations of dmit are as follows: DNA Only (blue), DNA and Fe(II) (red), 2.5 µM dmit (yellow) 5.0 µM dmit (green), 12.5 µM dmit (orange), 25 µM dmit (turquoise), 50 µM dmit (light blue). (B) Double reciprocal plot for the absorbances of calf thymus DNA and Fe(II) with varying concentrations of dmit. From this data, the binding constant was calculated to be -0.409. The equation was -3.0 + 7.34x and the R^2 value was 0.399.

Fe(II) had reacted in a similar manner as Zn(II) (see Fig. 6), with the increasing concentrations of dmit causing an increase in the absorbances of CT-DNA after binding a metal to it initially. In this case, the metal is Fe(II), and like Zn(II) it also decreases the absorbance of CT-DNA. Therefore, in the presence of metals, the dmit could be acting as a potential shield to the CT-DNA after comparing the absorbance values between adding a metal ion by itself versus adding a compound with it. Concerning the double reciprocal plot, the correlation is low

compared to the Zn(II) interaction, which could be due to Fe(II) ions being more concentrated than Zn(II) when bound to CT-DNA (as more noise occurs in the Fe(II) figure as opposed to the Zn(II) figure) which weakens the binding of dmit to CT-DNA directly. The binding constant is also negative, due to reasons previously mentioned (an insufficient method used to calculate the binding constant).

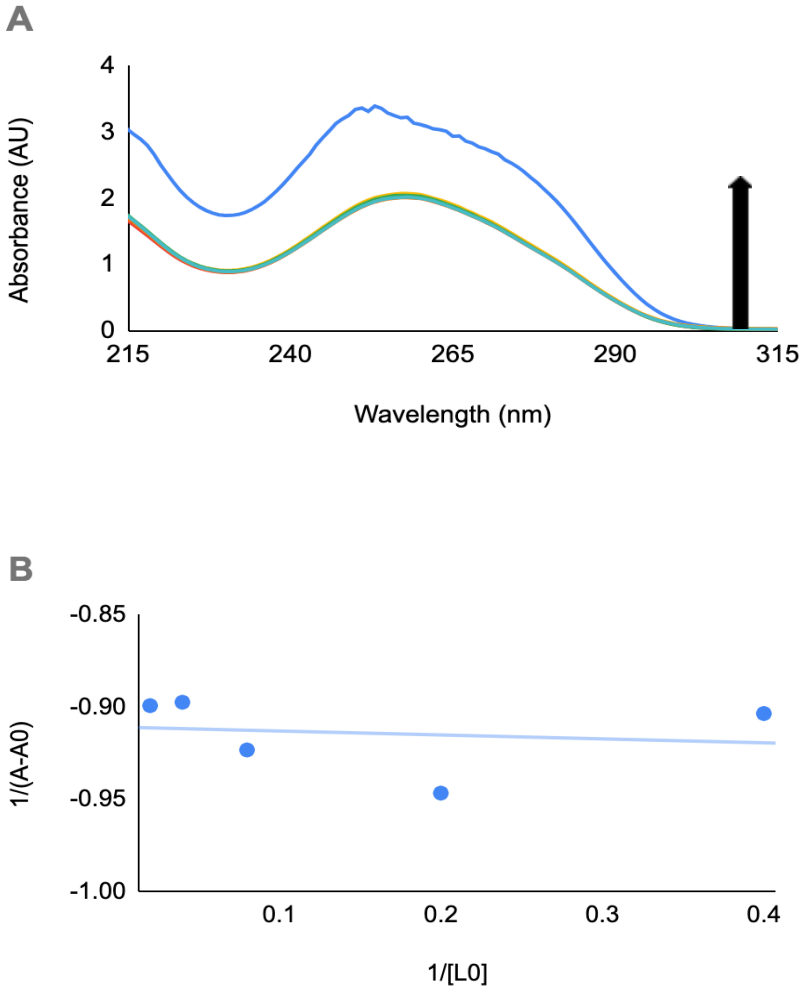

Fig. 8. (A) Absorbances of calf thymus DNA with varying concentrations of GSH. The concentrations of the added amounts of GSH are as follows: DNA Only (blue), 5.0 µM GSH (red) 10 µM GSH (yellow), 15 µM GSH (green), 20 µM GSH (orange), 25 µM GSH (turquoise). (B) Double reciprocal plot for the absorbances of calf thymus DNA with varying concentrations of GSH. From this data, the binding constant was calculated to be 42.8. The equation was -0.911 - 0.0213x and the R^2 value was 0.026.

GSH, like dmit and dmise (see Fig. 3 and Fig. 5) had caused the absorbance of CT-DNA to decrease at first, but as the concentration of the GSH in the CT-DNA had increased, the absorbance of the CT-DNA had also increased. It is difficult to differentiate between what spectra belong to what concentration because the gap between varying concentrations was too small. In Fig. 9 however (when Zn(II) is added to CT-DNA before the addition of GSH) this correlation will be much more readable. Concerning the double reciprocal plot of this spectra, the correlation is very low while the binding constant is the greatest value compared to the previous experiments. The binding constant value could be due to the fact that GSH binds strongly to CT-DNA, but because the points were very precise (because the intervals of the GSH concentrations were too close together), this left more room for the trendline to have a greater susceptibility for the correlation to be lower.

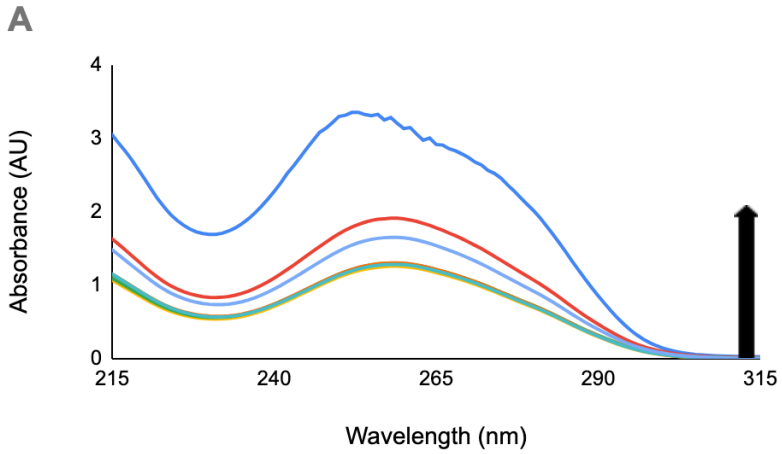

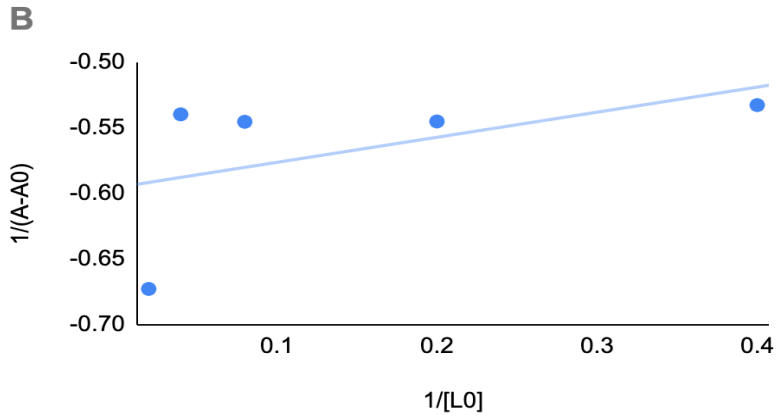

Fig. 9. (A) Absorbances of calf thymus DNA and Zn(II) with varying concentrations of GSH. The added amounts of the ion/complex as well as the concentrations of GSH are as follows: DNA Only (blue), DNA and Zn(II) (red), 5.0 μM GSH (yellow) 10 μM GSH (green), 15 μM GSH (orange), 20 μM GSH (turquoise), 25 μM GSH (light blue). (B) Double reciprocal plot for the absorbances of calf thymus DNA and Zn(II) with varying concentrations of GSH. From this data, the binding constant was calculated to be -3.12. The equation was $-0.595 + 0.191x$ and the R^2 value was 0.257.

Compared to Fig. 8, the absorbances of the varying GSH concentrations are much easier to differentiate due to the addition of Zn(II). Because the highest noticeable absorbance for GSH added is the highest concentration (50 μM), this indicates that the rest of the GSH absorbance values had increased upon increasing concentration. The gap between CT-DNA by itself and after the addition of Zn(II) however had increased (or the absorbance of CT-DNA after the addition of GSH had decreased more than the Zn(II) concentration. This was probably due to the fact that GSH needs to be more concentrated when added to CT-DNA in order to make beneficial changes to the absorbance of CT-DNA. Concerning the double reciprocal plot, the correlation was greater than that of GSH by itself, due to the separation of the absorbances from the addition of Zn(II). The binding constant was negative due to the reasons previously mentioned above (an insufficient method used to calculate the binding constant).

Conclusion

As expected, decreasing DNA concentration can be explained through the binding of Zn(II) with the structure of DNA, as the interaction of a metal ion to DNA is said to produce radicals that damage DNA.[17] It was also expected that iron-mediated damage of DNA would experience random fragmentation when bounded to its structure, which was shown in Fig. 7.[18]

Meanwhile, dmit, dmise, and GSH were shown to increase the absorbance of DNA and protect it from the metal ions. Despite how GSH did not overcome the Zn(II) barrier in the experiments, with greater concentrations to test with, it should be able to do so. Therefore overall, GSH, dmit, and dmise may be contributing factors to the science of working to develop supplements to help with cell death and to protect DNA from metal ions. Because the diversity of transition metal complexes is growing in terms of coordination numbers, geometries, redox potentials, and kinetic and thermodynamic characteristics, then understanding the bindings of other antioxidant compounds and complexes such as metal chelators, ergothioneine (ESH), and Ru (III) thione complexes with redox inactive metals is essential.[19-23] The same can also be applied to metal ions/complexes by understanding the bindings of iron derivatives such as iron-Salen complexes.[25]

Future Work

Another indicator to consider is hyperchromism, which is consistent with groove binding and can therefore indicate the unwinding of the DNA double helix when the binding is breaking apart.[18] Expanding to use multiple other methods such as CD spectroscopy, fluorescence spectroscopy, and viscous measurements using an Ostwald viscometer would also help prove the stability of the results. The binding modes can also be better predicted in this manner.

Author Information

Corresponding Author

Jacob Alewine – *Clemson University, Clemson, South Carolina 29634, United States.*

Email: alewin3@clemson.edu

Author Contributions

Julia L. Brumaghim - *Clemson University, Clemson, South Carolina 29634, United States.*

Funding Sources

This work was supported by a Grant from the National Science Foundation (NSF) No. 0525474.

Acknowledgements

The financial support by the NSF as well as the previous works of the members of the Brumaghim Research Group are highly acknowledged.

Abbreviations

Dmit, N, N'-dimethyl imidazole thione; Dmise, N, N'-dimethyl imidazole selone; CT-DNA, calf thymus-deoxyribonucleic acid; UV-Vis, Ultraviolet-Visible; MOPS, 3-morpholinopropane-1-sulfonic acid; GSH, glutathione; ESH, ergothioneine.

References

1. Barone, G.; Terenzi, A.; Lauria, A.; etc. *Coord. Chem. Rev.* **2013**, *257*, 2848-2862.
2. Silvestri, A.; Barone, G.; Ruisi, G.; etc. *J. Inorg. Biochem.* **2007,** *101,* 841-848.
3. Beraldo, H.; Garnier-Suillerot, A.; Tosi, L.; etc. *Biochem.* **1985,** *24,* 284-289.
4. Rasmussen, J.; Martinez, E.; Louka, P.; etc. *Expert Opin. Drug Deliv.* **2010,** *7,* 1063-1077.
5. Kumar, S.; Kesavan, M.; Kumar, G.; etc. *J. Mol. Struct.* **2018,** *1153,* 1-11.

6. Liu, S.; Cao, W.; Yu, L.; etc. *Dalton Trans.* **2013,** *42,* 5932-5940.
7. Hart, W.; Marczak, S.; Kneller, A.; etc. *J. Inorg. Biochem.* **2013,** *125,* 1-8.
8. Zimmerman, M.; Bayse, C.; Ramoutar, R.; etc. *J. Inorg. Biochem.* **2015,** *145,* 30-40.
9. Henle, E.; Linn, S. *J. Bio. Chem.* **1997,** *31,* 19095-19098.
10. Stadelman, B.; Murphy, J.; Owen, A.; etc. *Inorg. Chim. Act.* **2020,** *502,* 1-9.
11. Tarushi, A.; Psomas, G.; Raptopoulou, C.; etc. *J. Inorg. Biochem.* **2009,** *103,* 898-905.
12. Topala, T.; Bodoki, A.; Oprean, L.; etc. *Farmacia.* **2014,** *62,* 1049-1061.
13. Mudasir; Yoshioka, N.; Inoue, H. J. *Inorg. Biochem.* **1999**, *77*, 239-247.
14. Meneghini, R. *Elsevier Sci.* **1997,** *23,* 783-792
15. Forman, H. J.; Zhang, H.; Rinna, A. *Mol. Aspects of Med*. **2009**, *30*, 1-12.
16. Kalaras, M. D.; Richie, J. P.; Calcagnotto, A.; etc. *Food Chem.* **2017,** *233*, 429-433.
17. Nejdl, L.; Ruttkay-Nedecky, B.; Kudr, J.; etc. *Intern. J. Bio. Macro.* **2014,** *64,* 281-287.
18. Enright, H.; Miller, W.; Hebbel, R. *Ox. Uni. Press.* **1992,** *20,* 3341-3346.
19. Kathiresasn, S.; Anand, T.; Mugesh, S.; etc. *J. Photochem. Photobio. B: Bio.* **2015,** *148,* 290-301.
20. Pages, B.; Ang, D.; Wright, E.; etc. *Royal Soc. Chem.* **2015,** *44,* 3489-3878.
21. Goodman, S. C., Jr. Ph.D. Dissertation, Clemson University, Clemson, SC, 2019.
22. Mello-Filho, A.; Meneghini, R. *Elsevier Sci.* **1991,** *251,* 109-113.
23. Abbas, M. A. Ph.D. Dissertation, Clemson University, Clemson, SC, 2019.
24. Silvestri, A.; Barone, G.; Ruisi, G.; etc. *J. Inorg. Biochem.* **2004,** *98,* 589-594.